Mansoura Journal of Chemistry, vol. 32 (1), June, 2005.

SYNTHESIS, GEOMETRY AND ELECTRONIC SPECTRAL BEHAVIOUR OF MODIFIED NATURAL FUROCOUMARINS : ALLYLOXYXANTHOTOXIN AND ALLOXANTHOTOXIN

Eman El-Gendy[a] and Mamdouh Soliman[b]

a: Faculty of Specific Education Mansoura University, Mansoura, Egypt.

b: Chemistry Department – Faculty of Science – Mansoura University – Mansoura –Egypt.

(Received: 7 / 3 / 2005)

ABSTRACT

9-Allyloxyfuro[3,2-g][1]benzopyran-2-one (allyloxyxanthotoxin) (**3**) can be obtained by refluxing a mixture of xanthotoxol, allyl bromide and anhydrous potassium carbonate for 6 hours. On the other hand, when allyloxyxanthotoxin was fused at 150°C, it gave 4-allyl-9-hydroxyfuro[3,2-g][1]benzopyran-2-one(alloxanthotoxin)(**4**). The same product **4** was obtained when allyloxyxanthotoxin (**3**) was irradiated with ultra violet light at room temperature for 100 hours. The ground state molecular geometry of allyloxyxanthotoxin and alloxanthotoxin were theoretically investigated and optimized using ab-initio quantum mechanical level of computation.The electronic absorption spectra of allyloxyxanthotoxin and alloxanthotoxin have been investigated in different solvents with different polarities and the observed spectra were analyzed using Gaussian technique. The observed spectral bands were discussed and assigned to different transitions between molecular orbitals on the basis of the results of ZINDO/S quantum mechanical method using the configuration interaction procedure .

INTRODUCTION

Furocoumarins (FC) in combination with UVA (Ultra Violet radiation with wave length between 300-400 nm.) are used for the treatment of numerous autoimmune and skin deseases **[Bethea et. al., (1999)]** involving inflammation **[Peters et. al., (2000)]**. Usually the photosensitizing effect of furocoumarins is accounted for by the ability of

intercalating between DNA bases and covalent binding to pyrimidine bases under UVA irradiation **[Dall'Acqua et. al., (1979)]**.

Photooxygenation of furocoumarins : imperatorin (A) and alloimperatorin (B) gave the corresponding hydroperoxides (A' & B') **[Abou-Elzahab et. al., (1991)]**, which are used for damaging DNA photochemically of UVA (365 nm) **[Epe et. al., (1993)]** (Scheme 1).

The distribution profile of naturally-occurring furocoumarins shows large variations according to the plant species. *Rutaceae* **[Zobel and Brown, (1989)]**, *Moraceae* **[Swain and Downum, (1991)]**, *Leguminosea* **[Zobel et. al., (1991)]** and *Apiaceae* **[Abu-Mustafa et. al., (1970)]** families containing complex mixture of different furocoumarins such as xanthotoxin (8MOP), bergaptin (5MOP), psoralen (PS) and angilicine (AN) in large scales. Whereas, imperatorin (IMP) (A) and alloimperatorin (AIMP) (B) are present at low levels in some few species.

Here we have synthesized and investigated the two newly furocoumarins : allyloxyxanthotoxin (3) and alloxanthotoxin (4) from natural origin as imperatorin (A) and alloimperatorin (B) like respectively.

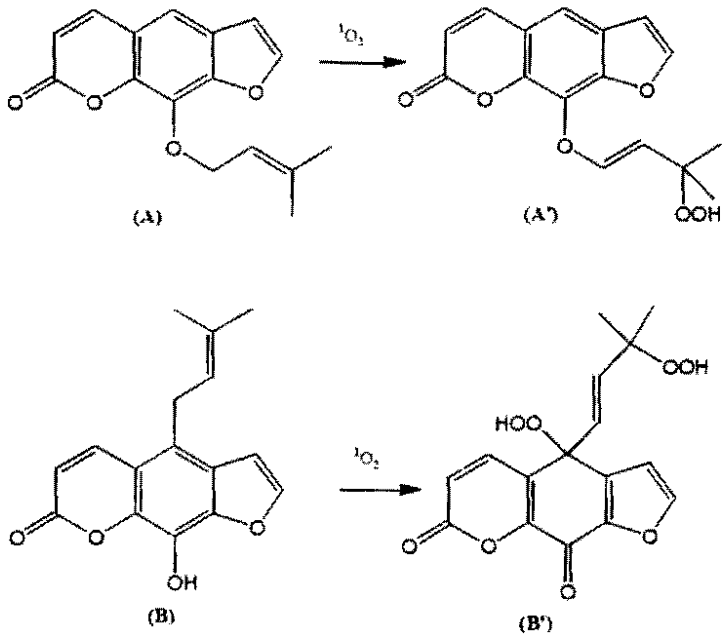

Scheme 1

Also, We found that it would be more convenient when we shed more light on the molecular geometry and the electronic structure and the spectral behaviour of these compounds to be the start point to investigate their possible interaction with DNA in a similar behaviour as reported with other furocomarins and similar compounds **[Jing-Xi Pan et. al., (2001)]**.

RESULTS AND DISCUSSION

The hydrolyzed derivative **(2)** was alkylated with allyl bromide to give 9-allyloxyfuro[3,2-g][1]benzopyran-2-one **(3)**, in a very good yield (80%) (Scheme 2).

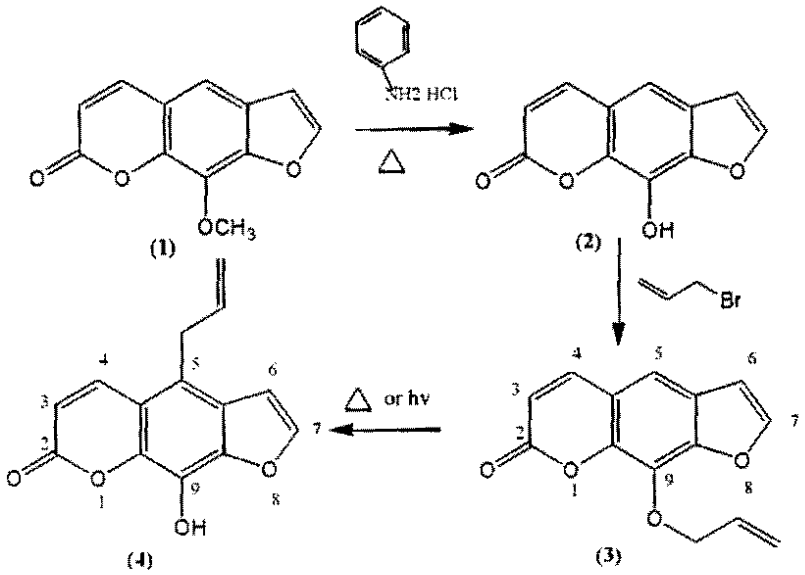

Scheme 2

^{1}H-NMR spectrum of **3** showed ABX system 5.45, 5.66 and 6.41 characteristic for vinylic group (CH_2=CH-) at the side chain. MS spectrum showed the molecular ion peak at m/z 242.

Just we performed the fusion of the allyloxy-derivative **(3)** the 4-allyl-9-hydroxyfuro[3,2-g][1]benzopyran-2-one **(4)** was formed. The same product **(4)** was obtained when the allyloxy-derivative **(3)** was photolyzed in chloroform solution, but in a poor yield (Scheme 2).

The mechanism of producing allo-derivative **(4)** was most likely formed through aromatic Claisen rearrangement. Where the allyl group underwent one inversion to give an ortho-isomer and another to give a para-isomer *via* [3,3] sigmatropic rearrangement, followed by [1,5] H shift (Scheme 3).

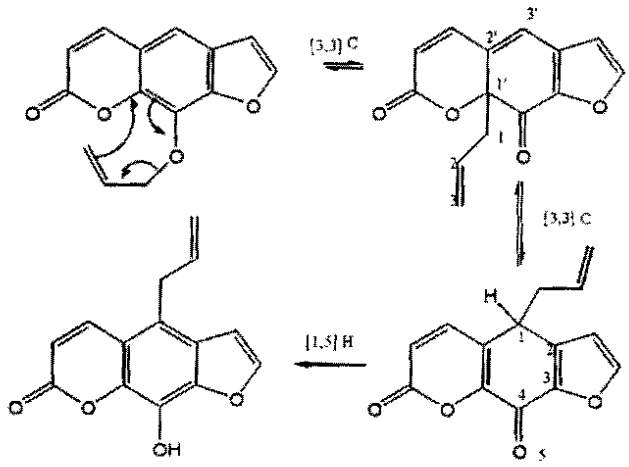

Scheme 3

^{1}H-NMR spectrum of **4** showed the hydroxyl proton at δ = 7.52 and the allyl group at δ 5.14, 5.35 and 6.21. MS spectrum of **4** showed the molecular ion peak at m/z 242 and the molecular ion peak minus a phenolic proton at 241 (base peak, 100%).

Ground State Geometry:

a) Geometry of allyloxyxanthotoxin (3)

The equilibrium state geometry of allyloxyxanthotoxin compound (3) was determined from the ab-initio optimization process using the 6-31G* basis set. The molecule showed in general that the three fused rings are exactly co-planar (see spatial representation and atomic numbering order in Fig. 1). The -O-CH_2-CH=CH_2 side chain is generally oriented out of the rings-plane so that the dihedral angle C_4-C_{11}-O_{12}-C_{16} (twisting about the C_{11}-O_{12}) was found to be about 79 degrees and inclined towards the coumarin moiety. The potential energy curve resulted from twisting the -O-CH_2-CH=CH_2 side chain about the C_{11}-O_{12} bond is given in fig.2a. Moreover, the terminal CH_2=CH-CH_2- was not oriented to be exactly in a trans direction relative to the C_{11}-O_{12} bond. Calculation of

the change in molecular total energy when CH_2=CH-CH_2- group is rotated about the O_{12}-C_{16} bond showed that the lowest energy is detected at a C_{11}-O_{12}-C_{16}-C_{17} dihedral angle of 168 degrees. This indicates that the CH_2=CH-CH_2- is twisted by an angle of 12 degrees from the trans orientation relative to the C_{11}-O_{12} bond. The potential energy curve arised from rotating the CH_2=CH-CH_2- group about the O_{12}-C_{16} bond presented in fig.2b. On the other hand, the terminal CH_2=CH- group of the side chain is twisted so that the dihedral angle O_{12}-C_{16}-C_{17}=C_{18} was about -154 degrees, which indicates that this terminal group is twisted from the trans- direction relative to the O_{12}-C_{16} bond by an angle of 26 degrees and inclined towards the furan moiety. The potential enrgy curve resulted from rotating the terminal part CH_2=CH- of the side chain about the C_{16}-C_{17} bond is shown in fig.2c.

Results of molecular orbital calculations indicated that the allyloxyxanthotoxin (3) molecule is a strong dipole and has a dipole moment of 7.52 Debye. The calculated atomic charges indicated that the ketonic and hydroxyl oxygen atoms O_7 and O_{12} are the highest negative centers among all atoms. Atomic charges of some active centers as well as bond lengths and orders of the important bonds are summarized in table 1.

Table(1): Atomic charges and bond lengths and orders of some important atoms and bonds of allyloxyxanthotoxin (3) as resulted from molecular orbital calculations.

Atom	Charge	Bond	Length (Å)	Order
Coumarin moiety				
O_5	-0.286	C4-O5	1.374	0.751
O_7	-0.328	O5-C6	1.376	0.741
		C6=O7	1.206	1.816
Furan Moiety				
O_{13}	-0.247	O_{10}-O_{13}	1.366	0.794
		O_{13}-C_{14}	1.388	0.796
Side Chain				
O_{12}	-0.333	C_{11}-C_{12}	1.362	0.883
C_{16}	0.032	O_{12}-H_{16}	1.457	0.684

energy of ψ_{45} (HOMO) = -8.181 eV : energy of ψ_{46} (LUMO) = -0.635 eV

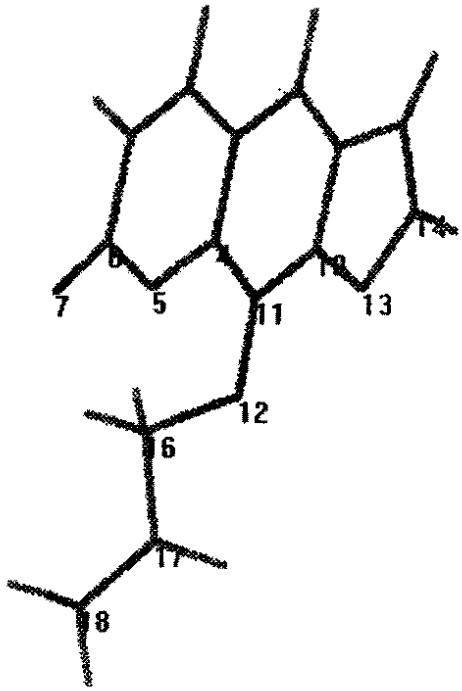

Fig.(1): Spatial representation of allyloxyxanthotoxin (3) obtained from geometry optimization and numbering order of its atoms.

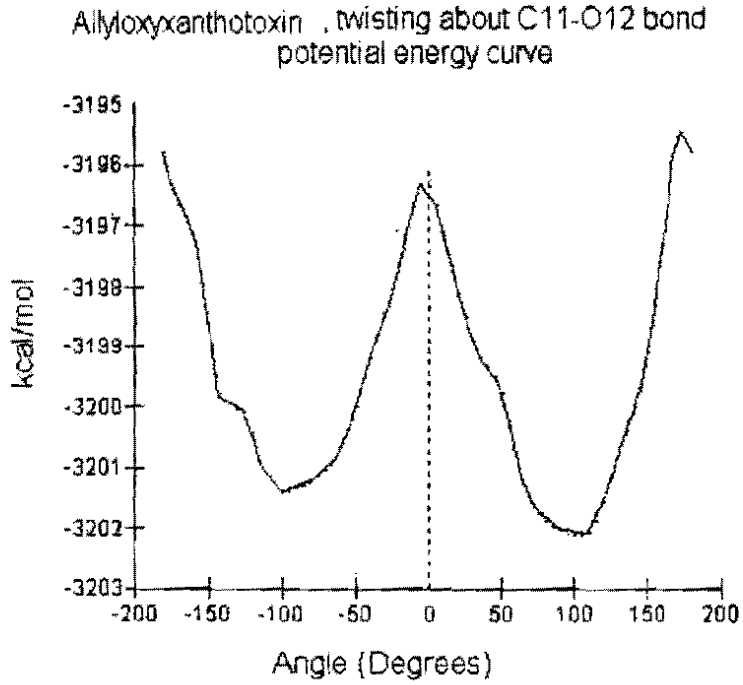

Fig. 2a : The potential energy curve resulted from twisting the side chain of allyloxyxanthotoxin (3) about C_{11}-O_{12} bond.

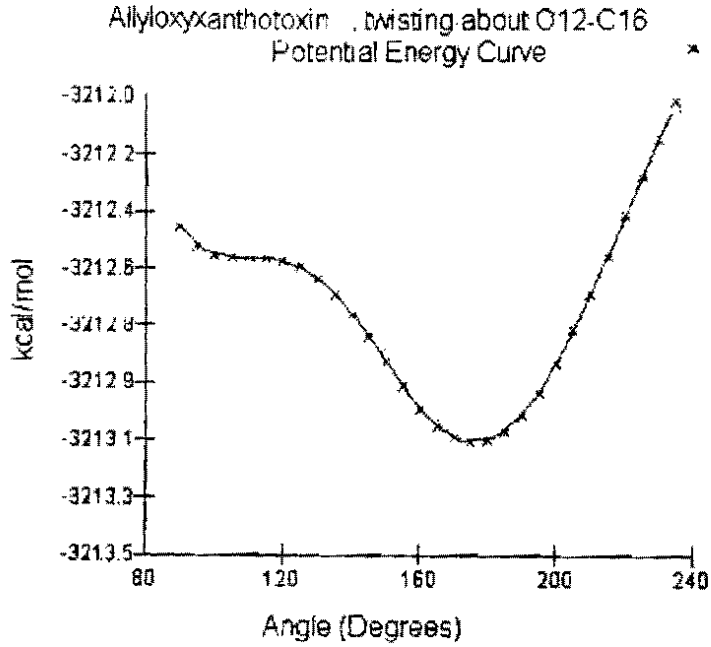

Fig. 2b: The potential energy curve of allyloxyxanthotoxin(3) side chain Twisting about O_{12}-C_{16} bond.

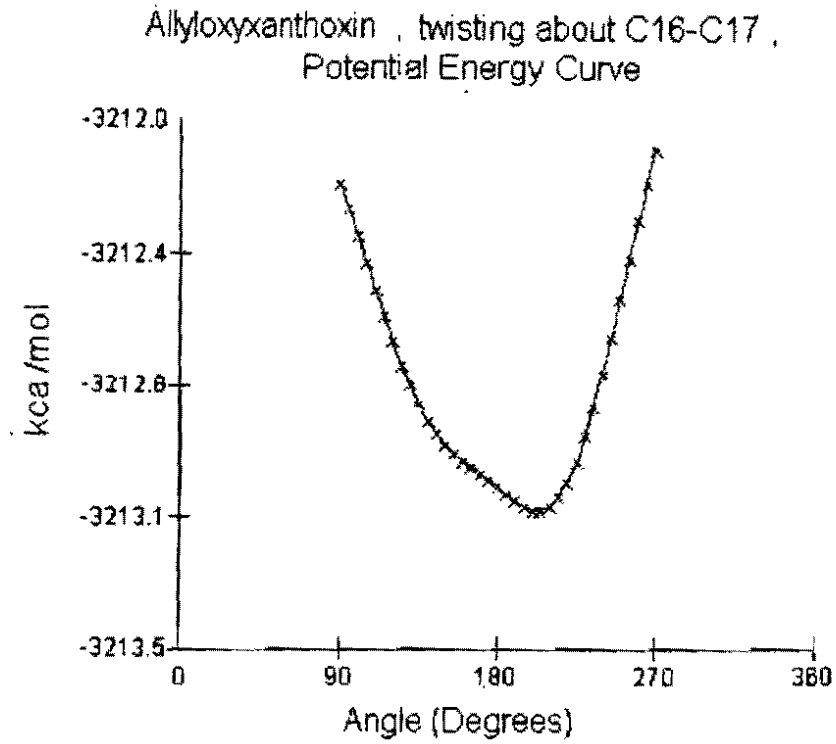

Fig. 2c : The potential energy curve resulted from twisting the terminal part CH_2=CH- of the side chain of allyloxyxanthotoxin(3) about the C_{16}-C_{17} bond.

b) Geometry of alloxanthotoxin:

The equilibrium ground state geometric parameters of alloxanthotoxin compound (**4**) was also obtained from the geometry optimization process using the ab-initio method using the 6-31G* basis set. Results showed that the three fused rings of the molecule, as in case of allyloxyxanthotoxin (**3**) are exactly coplanar. The CH_2=CH-CH_2- side chain on the other hand, is oriented out of the rings-plane so that the dihedral angle C_9-C_8-C_{16}-C_{17} (see atomic numbering order in Fig.3) was found to be about 80 degrees, and inclined towards the furan moiety of the molecule. The potential energy curve arised from rotation of the CH_2=CH-CH_2- side chain about the C_8-C_{16} bond, out of the molecular plane, is shown in Fig.4a. The terminal -CH=CH_2 group of the side chain was found to be twisted from the trans orientation relative to the C_8-C_{16} bond. The calculated C_8-C_{16}-C_{17}=C_{18} dihedral angle was found to be -121 degrees. This means that this group is twisted from the trans

direction relative to the C_8-C_{16} bond by an angle of 59 degrees and inclined towards the coumarin moiety of the molecule (see Fig.1). The potential energy curve arised as a result of twisting of the terminal –$CH=CH_2$, about C_{16}-C_{17} is given in fig.4b. The phenolic OH- group, on the other hand was found to be exactly coplanar with the rings-plane and H-atom is directed towards the coumarin moiety of the molecule. The potential energy curve of twisting the OH- group about the C_{11}-O_{12} bond, out of the molecular plane is shown in fig.4c.

Moreover, results of molecular orbital calculations indicated that the alloxanthotoxin (**4**) molecule is a stronger dipole than allyloxyxanthotoxin (**3**), and has a dipole moment of 7.73 Debye. The calculated atomic charges indicated that the ketonic and hydroxyl oxygen atoms O_7 and O_{12} are the highest negative centers amoung all atoms in the molecule. Atomic charges of some active centers as well as bond lengths and orders of the important bonds are summarized in table 2.

Table (2): Atomic charges and bond lengths and orders of some important atoms and bonds of Alloxanthotoxin as resulted from molecular orbital calculations.

Atom	Charge	Bond	Bond Length (Å)	Bond Order
Coumarin moiety				
O_5	-0.2911	C4-O5	1.382	0.739
O_7	-0.3317	O5-C6	1.378	0.758
		C6=O7	1.212	1.816
Furan Moiety				
O_{13}	-0.2404	O_{10}-O_{13}	1.388	0.785
		O_{13}-C_{14}	1.387	0.812
Phenolic OH-Group				
O_{12}	-0.3736	C_{11}-C_{12}	1.364	0.911
H_{21}	0.049	O_{12}-H_{21}	0.949	0.753

Energy of ψ_{45} (HOMO) = -8.117 eV ; Energy of ψ_{46} (LUMO) = -0.702 eV

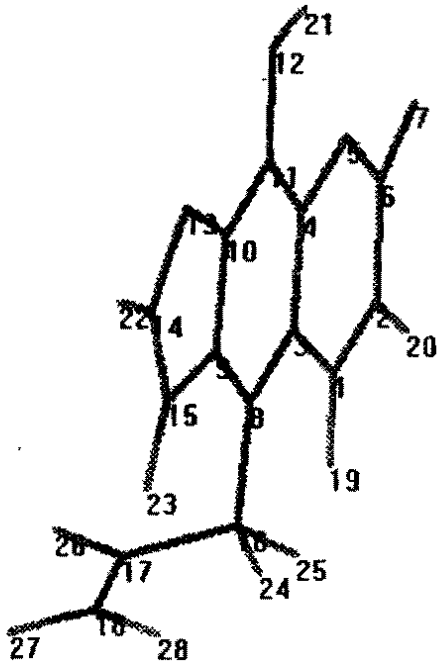

Fig. (3): Spatial representation of alloxanthotoxin(4) as obtained from geometry optimization and numbering order of its atoms.

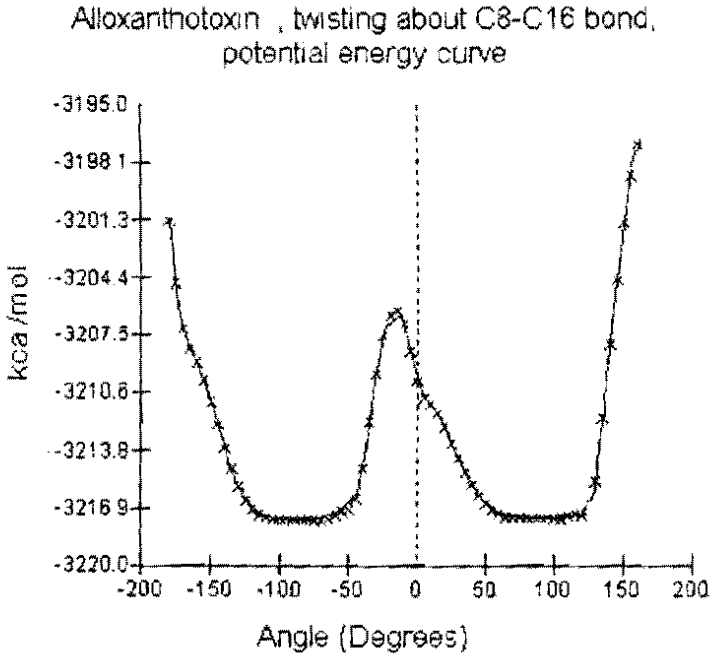

Fig. 4a: The Potential energy curve of twisting the side chain of alloxanthotoxin (4) about C_8-C_{16} bond.

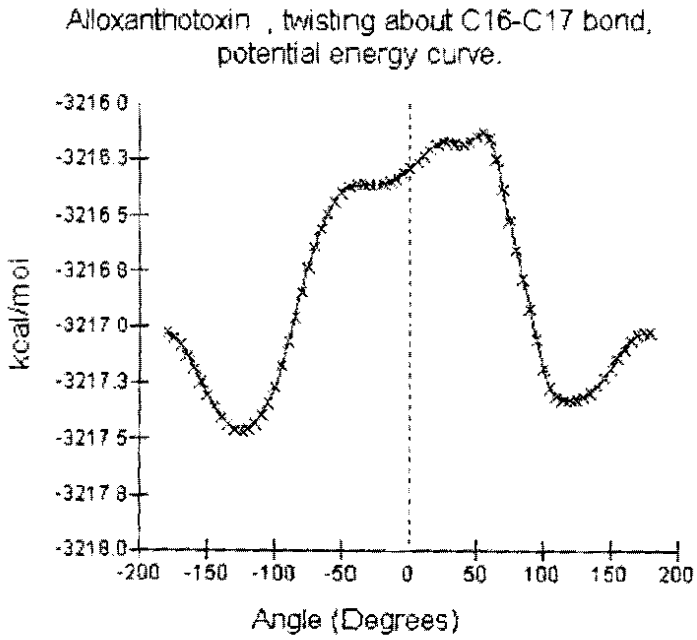

Fig. 4b: Potential energy curve of twisting the terminal $-CH=CH_2$ part of the side chain of alloxanthotoxin (4) about C_{16}-C_{17} bond.

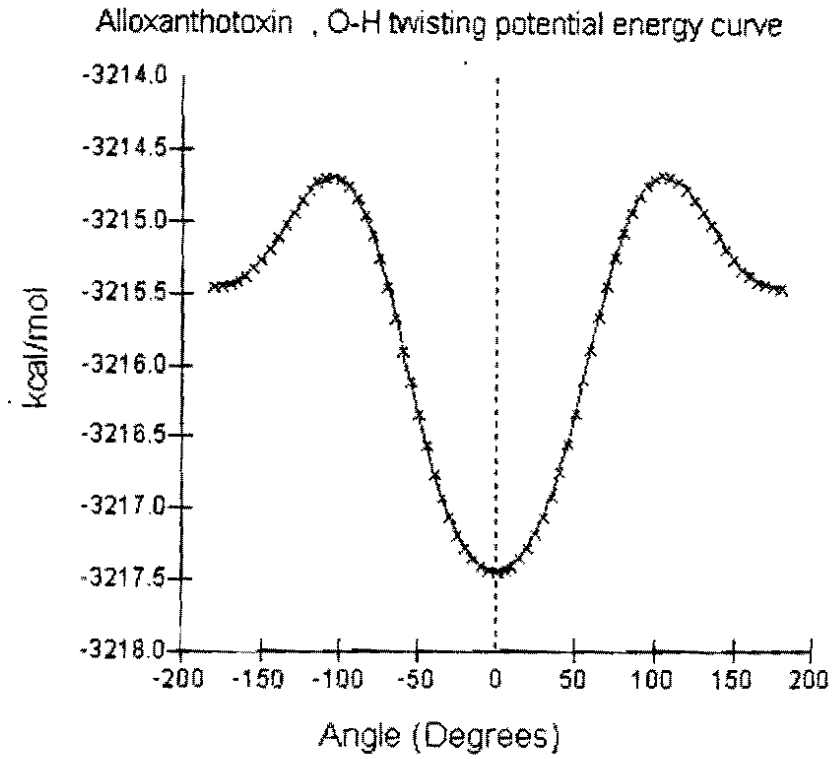

Fig. 4c : Potential energy curve of twisting of phenolic OH- group of alloxanthotoxin (4) about the C_{11}-C_{12} bond.

Electronic Absorption Spectra:

a) Electronic Spectra of allyloxyxanthotoxin (3)

The electronic absorption spectra of the allyloxyxanthotoxin (**3**) in different solvents are given in Fig.5. The absorption bands in the spectrum in the region from 250-400 nm, in the different solvents, appeared in three different regions of the spectrum at 250-275, and 275-330 and at 330-380 nm. The region 275-330 nm was observed to be composed of different overlapped absorption bands. We carried out the configuration interaction calculations for electronic transitions between the five highest occupied ψ_{41}-ψ_{45}, and the five lowest vacant ψ_{46}-ψ_{50} MO's using ZINDO/S method. Results of calculation of electronic transitions showed that there are four absorption bands expected in the concerned region of electronic spectrum. On these bases, the observed bands are subjected to Gaussian Peak-Analysis and curve fitting with the aid of the Microcal ORIGIN software[18]. The observed bands in the

different regions were analyzed to their expected four components and their characteristics such as Einstein's probability coefficients, life-time of the .excited states and oscillator strengths were determined. The analysed spectra with the Gaussian curve fitting are given in Fig.6. The experimentally observed band maxima, with their estimated molar extinction coefficients and oscillator strengths in different solvents are summarized in table 3. The different absorptions were assigned to electronic transition on the basis of the calculated molecular orbitals and configuration interaction results. The wavefunctions (ψ_{43}-ψ_{48}) of these MO's with their energies as obtained from ZINDO/S MO calculations are presented in Fig.7. The CI state-functions of the excited states and the corresponding transition energies and oscillator strength as resulted from CI calculations are depicted in table 4.

When we take the spectrum in n-hexane as a nonpolar solvent to discuss our results, we found that the first observed band was detected at 340 nm with molar extinction of ε=2900. This band is considered to be some kind of n-π^* transition, between the occupied ψ_{44} and ψ_{45} orbitals to the vacant ψ_{46} and ψ_{47} orbitals. Calculations showed that these two orbitals have their highest contribution from atomic orbitals of the oxygen atoms of the coumarine moiety (ψ_{45}) and furan moiety (ψ_{44}), and both have considerable contribution from π- orbitals located on coumarin moiety. The vacant ψ_{46} and ψ_{47} orbitals on the other hand have their main contribution from the π-orbitals located at the coumarin moiety in ψ_{46} and on the furan moiety in ψ_{47}. The observed oscillator strength of this band has a value of 0.017 which characterizing a forbidden transition.

The second observed band was detected at 312 nm with molar extinction of ε=4400. It is also a n-π^* transition and attributed to transition between the occupied ψ_{41} which has its highest weight of contribution from the atomic orbitals of the ketonic oxygen of the coumarin moiety, and the unoccupied ψ_{46} orbitals which is mainly contributed from the π-orbitals localized at the coumarin moiety. It was also observed as expected with a very weak intensity and oscillator strength of 0.025. The estimated Einstein probability coefficients (absorption and emission) and the life-time of the excited states of these two bands have values of the order 10^7 (sec^{-1}) for both absorption and emission ($sec^{-1}.g^{-1}$) transition probabilities and values of the order 10^{-7} seconds for life-time of the excited states. This interprets the weakness

and broadness of such bands in the UV spectrum. The calculated values of the oscillator strength of these bands obtained from the ZINDO/S-CI procedure are in agreement with the experimentally estimated values.

The third band of the spectrum (in n-hexane solvent) was that at 291 nm with molar extinction of ε=11400 .This band, as shown from table 2, is to high extent is a π-π^* transition and attributed to transition between the occupied ψ_{44} and ψ_{45} orbitals with their high contribution from π-orbitals to the vacant ψ_{46} and ψ_{47} which are mainly π-orbitals.

The fourth band in the spectrum was obtained at 261 nm with molar extinction coefficient of ε=13300. This transition is also a kind of π-π^* transition and arised due to possible transition between ψ_{44} and ψ_{45} and the vacant ψ_{46}, ψ_{47} and ψ_{48} orbitals as seen from table 4. The estimated Einstein probability coefficients from the observed band maxima and extinction coefficients of the third and fourth bands showed that these bands in general have absorption probabilities (sec^{-1}) as well as emission probability ($sec^{-1}.g^{-1}$) of the order 10^8 and life-time of excited states of the order 10^{-9} seconds. This indicates that these two bands are UV-observable more than than the first and second bands. The calculated oscillator strengths of the four bands from the CI job were found to be far higher than those experimentally estimated values.

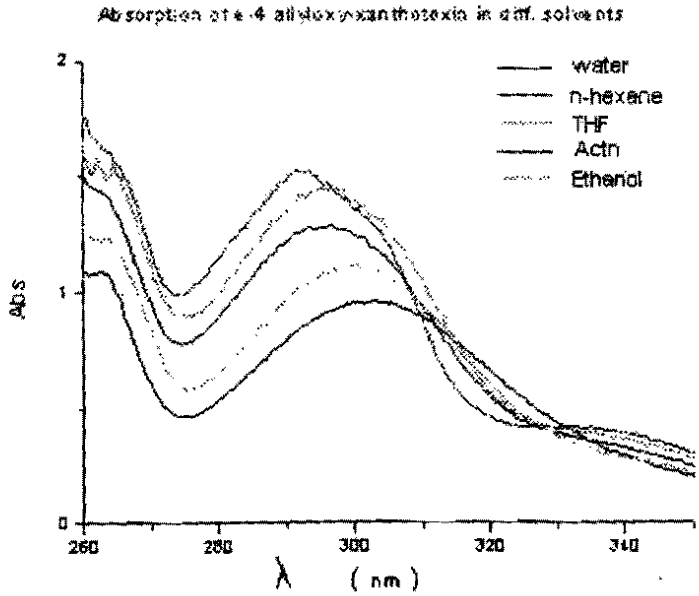

Fig.(5): Observed uv-spectra of allyloxyxanthotoxin (3) in different solvents.

Table (3): Observed bands of Allyloxyxanthotoxin in different solvents, their observed and calculated Oscillator strengths and their assignments.

Water			Ethyl alcohol			THF			n-hexane		
λ (nm)	ε L.mol^{-1}cm^{-1}	F(Osc)	λ (nm)	ε L mol^{-1}cm^{-1}	F(osc.)	λ (nm)	ε L mol^{-1}cm^{-1}	F(osc.)	λ (nm)	ε L.mol^{-1}cm^{-1}	F(osc.)
262	10800	0.056	262	11100	0.047	262	16800	0.138	261	13300	0.061
293	8500	0.062	292	7600	0.060	292	12000	0.064	291	11400	0.085
304	4500	0.027	305	5100	0.030	307	6900	0.029	312	4400	0.025
334	1500	0.008	334	2700	0.022	336	3900	0.035	340	2900	0.017

For the 1st and 2nd bands: Einstein's absorption coefficient (A_{if}) $\approx 10^{7}$, Einstein's absorption coefficient (B_{if}) $\approx 10^{7}$, Life-time $\approx 10^{-7}$

For the 3rd and 4th bands: Einstein's absorption coefficient (A_{if}) $\approx 10^{8}$. Einstein's absorption coefficient (B_{if}) $\approx 10^{8}$, Life-time $\approx 10^{-9}$

Table (4): Configuration Interaction state functions of the excited states and the corresponding transition energies (ΔE) and oscillator strength (f) for the Allyloxyxanthotoxin compound.

CI- results			Transition state	coefficients of state functions
λ (nm)	ΔE (eV)	F(osc.)		
254	4.860	0.776	ψ_{45} -ψ_{47} ψ_{45} -ψ_{48} ψ_{44} -ψ_{47} ψ_{45} -ψ_{46}	0.4370 0.3402 0.3555 0.2132
277	4.457	0.290	ψ_{45} -ψ_{47} ψ_{44} -ψ_{46} ψ_{45} -ψ_{46}	0.3176 0.5553 -0.2220
285	4.332	0.003	ψ_{41} -ψ_{46} ψ_{41} -ψ_{48}	0.6039 0.3524
320	3.858	0.080	ψ_{45} -ψ_{46} ψ_{45} -ψ_{48} ψ_{44} -ψ_{47}	0.5840 0.1713 0.3113

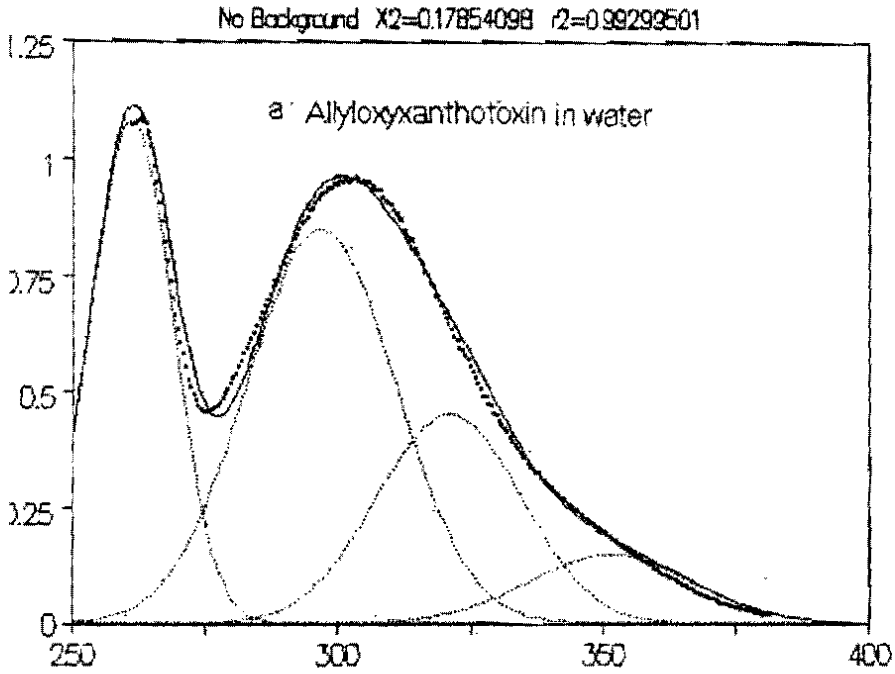
No Background X2=0.17854098 r2=0.99299501
a : Allyloxyxanthotoxin in water
1.25
1
0.75
0.5
0.25
0
250
300
350
400

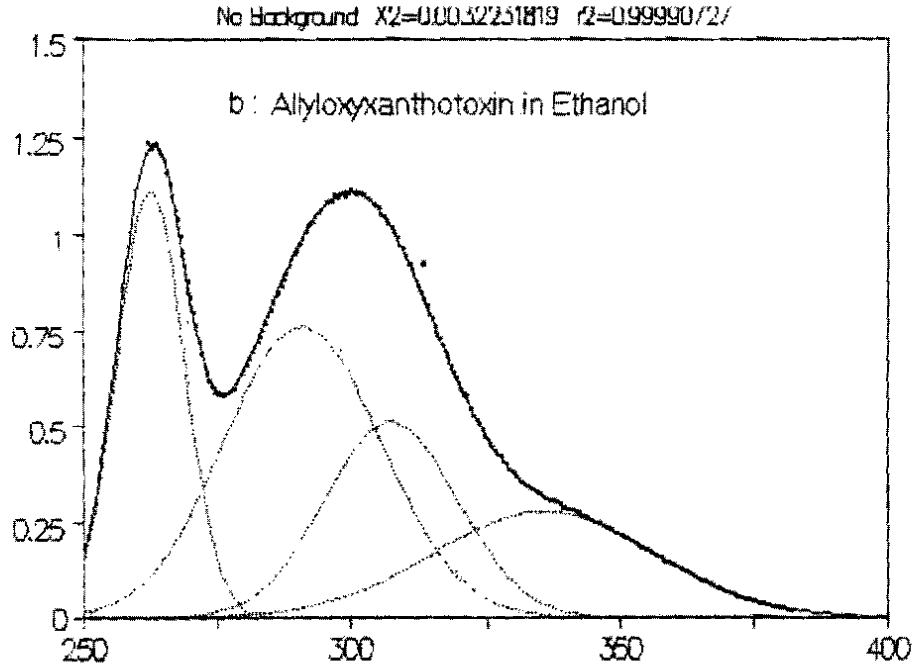
No Background X2=0.00522518819 r2=0.99999027
b : Allyloxyxanthotoxin in Ethanol
1.5
1.25
1
0.75
0.5
0.25
0
250
300
350
400

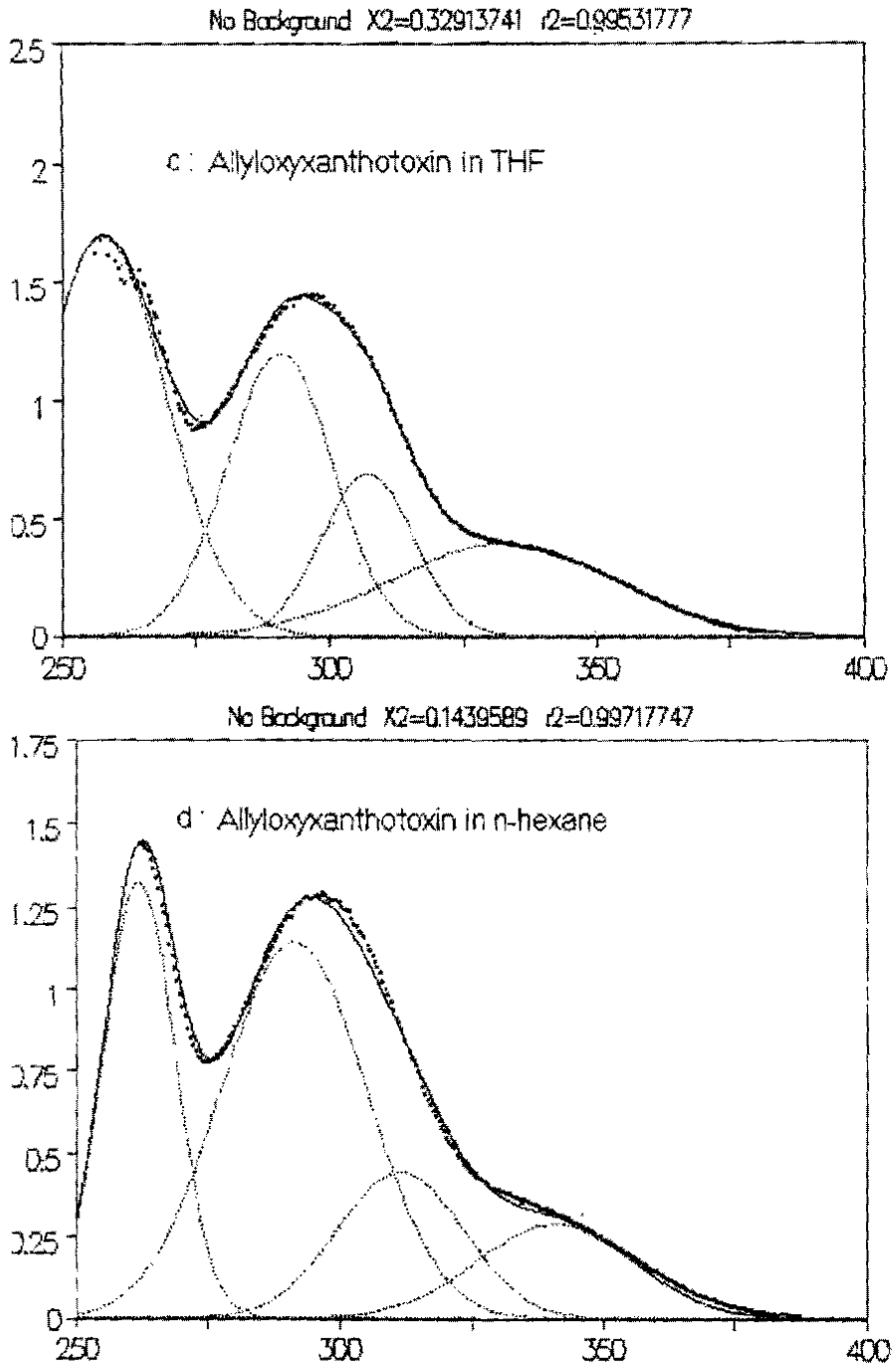

Fig 6a-d : Gaussian analysis of the UV-spectra of allyloxyxanthotoxin (3) in different solvents.

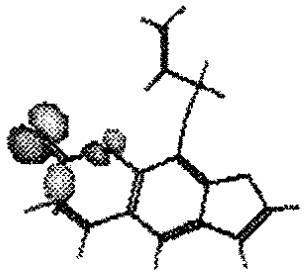

MO 41 E = - 10.160 eV

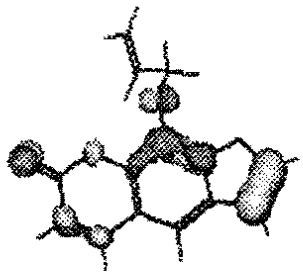

MO 42 E = - 10.022 eV

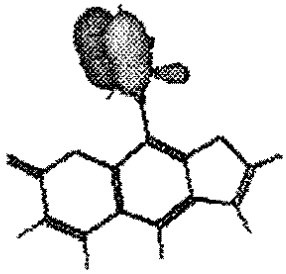

MO 43 E = - 9.546 eV

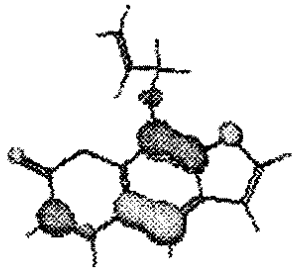

MO 44 E = - 8.506 eV

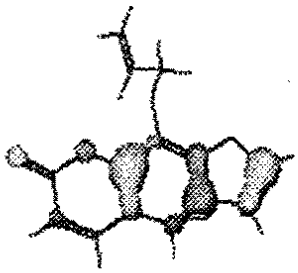

MO 45 E = - 8.181 eV

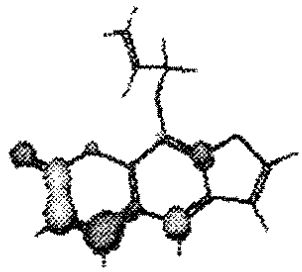

MO 46 E = - 0.635 eV

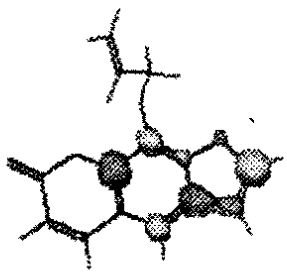

MO 47 E = - 0.016 eV

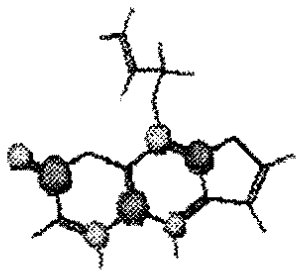

MO 48 E = 0.777 eV

Fig.(7): Representation of the calculated wavefunctions of the Molecular orbitals involved in the electronic transitions of Allyloxyxanthotoxin (3) . (Orbital contours higher than 0.07)

b) Electronic Absorption Spectra of alloxanthotoxin (4)

The electronic absorption spectra of the alloxanthotoxin (4) in different solvents are given in Fig. 8. The absorption bands in the spectrum in the region from 240-400 nm, in the different solvents, were appeared in three different regions of the spectrum at 250-285, and 285-330 and at 330-380 nm. Each of these regions seemed to be composed of different overlapped absorption bands. The configuration interaction calculations for electronic transitions between the five highest occupied ψ_{41}-ψ_{45} , and the five lowest vacant ψ_{46}-ψ_{50} MO's using ZINDO/S method showed that there are six absorption bands were expected in the measured region of electronic spectrum. On these bases, the observed bands are subjected to Gaussian Peak-Analysis and curve fitting. The observed bands in the different regions were analyzed to their expected six components and their characteristics (as Einstein's probability coefficients, half-life time of the excited states and oscillator strengths) were determined. The analyzed spectra with the Gaussian curve fitting are presented in Fig.9. The experimentally observed band maxima, with their estimated molar extinction coefficients and oscillator strengths in different solvents are summarized in table 5. The different absorptions were assigned to electronic transition on the basis of the calculated molecular orbitals and configuration interaction results. Configuration interaction results indicated that the highest two occupied and lowest three vacant molecular orbitals are those, which have the highest weight of contribution in the different transitions. The wave functions (ψ_{43}-ψ_{48}) of these MO's with their energies as obtained from ZINDO/S MO calculations are presented in Fig.10. The CI state-functions of the excited states and the corresponding transition energies and oscillator strength as resulted from CI calculations are depicted in table 6.

When we take the spectrum in n-hexane as a non-polar solvent to discuss our results, we found that the first observed band was detected at 363 nm with molar extinction of ε=2100. This band is attributed to n-π^* transition, between the occupied non-bonding ψ_{44} and ψ_{45} orbitals, which have high contribution from atomic orbitals of the oxygen atoms of the ketonic and hydroxyl group, and the vacant ψ_{46} and ψ_{47} π-orbitals located at the coumarin moiety in case ψ_{46} and on the benzenoid and furan ring in ψ_{47}. The observed oscillator strength of this band has a value of 0.012 characterizing a forbidden transition.

The second observed band was detected at 321 nm with molar extinction of ε=4500. It is also a n-π* transition and attributed to transition between the nonbonding ψ_{44} and ψ_{45} orbitals and the ψ_{46} and ψ_{47} π-orbitals. It was also observed as expected with a very weak intensity and oscillator strength of 0.017. The estimated Einstein probability coefficients (absorption and emission) and the life-time of the excited states of the first and second bands have values of the order 10^6 for both absorption (sec^{-1}) and emission ($sec^{-1}.g^{-1}$) transition probabilities and values of the order 10^{-6} seconds for life-time of the excited states. This indicated that these two bands are forbidden bands to be detected in the UV spectrum. The calculated values of the oscillator strength produced values, which are to some extent in agreement with the experimentally estimated values.

The third band was obtained at 310 nm with molar extinction coefficient of ε=16500 is also a n-π* transition attributed to the transition between the nonbonding ψ_{41} which has its main contribution from the non-bonding atomic orbitals of oxygen atoms of the (coumarin moiety, and the ψ_{46} and ψ_{47} π-orbitals. The estimated Einstein probability coefficients from the observed band maxima and extinction coefficients showed that this band has absorption probability (sec^{-1}) as well as emission probability ($sec^{-1}.g^{-1}$) of the order 10^7 and life-time of excited state of the order 10^{-7} seconds. This indicates that this band is more detectable than the first two bands. This band was detected with oscillator strength of 0.15, which is in agreement with the quantum mechanically calculated value (0.102).

The fourth band of the spectrum (in n-hexane) was that at 276 nm with molar extinction of ε=22200. This band, as shown from table 2, is to high extent a π-π* transition and attributed to transition between the occupied ψ_{44} and ψ_{45} orbitals to the vacant ψ_{46}, ψ_{47} and ψ_{48} which are mainly π-orbitals.

The fifth and sixth bands in the spectrum were obtained at 267 and 252 nm with molar extinction coefficient of ε=21900 and 26100 respectively. These are also a kind of π-π* transition. They arised due to possible transition between the occupied ψ_{44} and ψ_{45} and the vacant ψ_{47} ,ψ_{48} and ψ_{50} π-orbitals as seen from table 6. The estimated Einstein probability coefficients from the observed band maxima and extinction coefficients of the forth, fifth and sixth bands showed that these bands have absorption probabilities (sec^{-1}) as well as emission probability (sec^{-1}

$^{1}.g^{-1}$) of the order 10^{8} and life-time of excited state of the order 10^{-9} seconds. This indicates that these three bands are allowed and detectable other than the first three bands. The calculated oscillator strengths of these bands from the CI job were found to be higher than those experimentally estimated values by a factor of seven.

The effect of solvent polarity on the observed absorption bands generally appeared in the change of their positions as well as their intensities. In the spectrum of allyloxyxanthotoxin (**3**) as well as alloxanthotoxin (**4**), the increase of solvent polarity, showed no considerable shift (or a very weak blue shift) in case of the first two bands of allyloxyxanthotoxin (**3**) and the first three bands in case of alloxanthotoxin (4) (n-π^* bands) and no shift (or a very weak red shift) in case of the other π-π^* bands (see table 3 and 5). This very weak shift in band positions in both molecules can be ascribed to their strong dipole (Dipole moments are 7.52 and 7.73 Debye for allyloxyxanthotoxin (**3**) and alloxanthotoxin (**4**) respectively) and electron excitation may not cause any considerable decrease in the polar character of the molecule. Accordingly, the solvation energy of both the ground and the excited states will have no significant difference and consequently no considerable shift in band maxima with increasing solvent polarity could be observed.

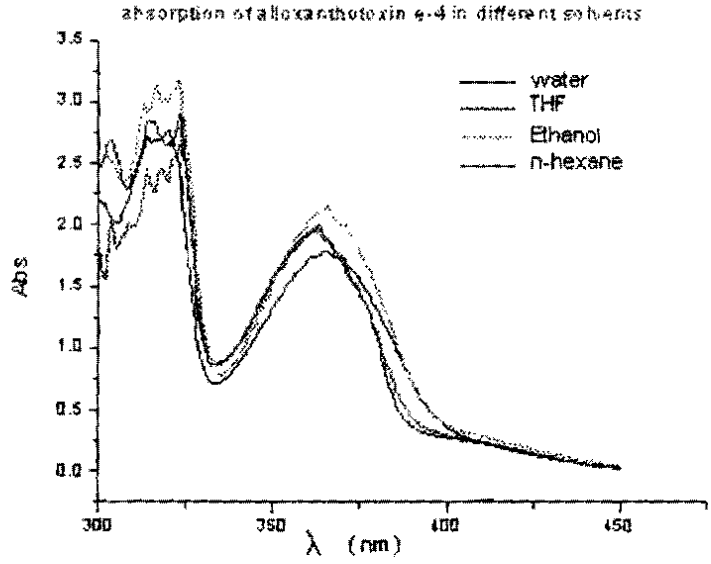

Fig. 8 : The observed uv-spectra of alloxanthotoxin (4) in different solvents.

Table (5): Observed band maxima,molar extinction coefficients (ε) and oscillator strengths (f) of alloxanthotoxin compound in different solvents

Water			Ethyl alcohol			THF			n-hexane		
λ (nm)	ε $L.mol^{-1}cm^{-1}$	f	λ (nm)	ε $L.mol^{-1}cm^{-1}$	f	λ (nm)	ε $L.mol^{-1}cm^{-1}$	f	λ (nm)	ε $L\ mol^{-1}cm^{-1}$	f
253	20600	0.070	252	٢٢٨٠٠	0.050	252	١٧١٠٠	0.087	252	26100	0.117
267	18600	0.054	267	٢١١٠٠	0.091	267	١٦٦٠٠	0.049	267	21900	0.057
275	23900	0.075	276	٢٧١٠٠	0.082	276	١٨٨٠٠	0.043	276	22200	0.051
311	16100	0.162	311	١٦٦٠٠	0.165	311	١١٨٠٠	0.145	310	16500	0.147
320	1800	0.006	321	٢٠٠٠	0.014	321	٤٧٠٠	0.029	321	4500	0.017
362	1300	0.006	363	٢٢٠٠	0.012	363	2000	0.011	363	2100	0.012

For the 1st , 2nd and 3rd bands : Einstein's absorption coefficient (A_{if}) $\approx 10^{6}$-10^{7} , Einstein's absorption coefficient (B_{if}) $\approx 10^{6}$-10^{7} , Life-time ($t_{1/2}$) $\approx 10^{-6}$-10^{-7}

For the 4th , 5th and 6th bands : Einstein's absorption coefficient (A_{if}) $\approx 10^{8}$, Einstein's absorption coefficient (B_{if}) $\approx 10^{8}$, Life-time ($t_{1/2}$) $\approx 10^{-9}$.

Table (6): Configuration Interaction state functions of the excited states and the corresponding transition energies (ΔE) and oscillator strength (f) for the alloxanthotoxine compound.

CI- results			Transition state	Coefficients of state coefficient
λ (nm)	ΔE (eV)	F(osc)		
233	5.298	0.511	$(\Psi_{45})^{-1}\ \Psi_{48}$ $(\Psi_{44})^{-1}\ \Psi_{47}$ $(\Psi_{45})^{-1}\ \Psi_{50}$ $(\Psi_{44})^{-1}\ \Psi_{48}$	0.539 0.361 0.156 0.135
262	4.712	0.481	$(\Psi_{44})^{-1}\ \Psi_{47}$ $(\Psi_{45})^{-1}\ \Psi_{47}$ $(\Psi_{45})^{-1}\ \Psi_{48}$ $(\Psi_{44})^{-1}\ \Psi_{46}$ $(\Psi_{44})^{-1}\ \Psi_{48}$	-0.416 -0.389 0.237 -0.148 0.114
269	4.589	0.653	$(\Psi_{45})^{-1}\ \Psi_{47}$ $(\Psi_{45})^{-1}\ \Psi_{46}$ $(\Psi_{45})^{-1}\ \Psi_{48}$ $(\Psi_{44})^{-1}\ \Psi_{47}$ $(\Psi_{44})^{-1}\ \Psi_{46}$	0.488 0.273 0.261 -0.213 0.134
295	4.185	0.102	$(\Psi_{41})^{-1}\ \Psi 46$ $(\Psi_{41})^{-1}\ \Psi_{47}$	0.597 0.362
310	3.982	0.034	$(\Psi_{44})^{-1}\ \Psi_{46}$ $(\Psi_{45})^{-1}\ \Psi_{47}$ $(\Psi_{44})^{-1}\ \Psi_{47}$	0.660 0.199 0.106
355	3.477	0.011	$(\Psi_{45})^{-1}\ \Psi_{46}$ $(\Psi_{44})^{-1}\ \Psi_{47}$ $(\Psi_{45})^{-1}\ \Psi_{48}$ $(\Psi_{45})^{-1}\ \Psi_{47}$ $(\Psi_{44})^{-1}\ \Psi_{50}$	0.574 0.320 0.171 0.103 0.101

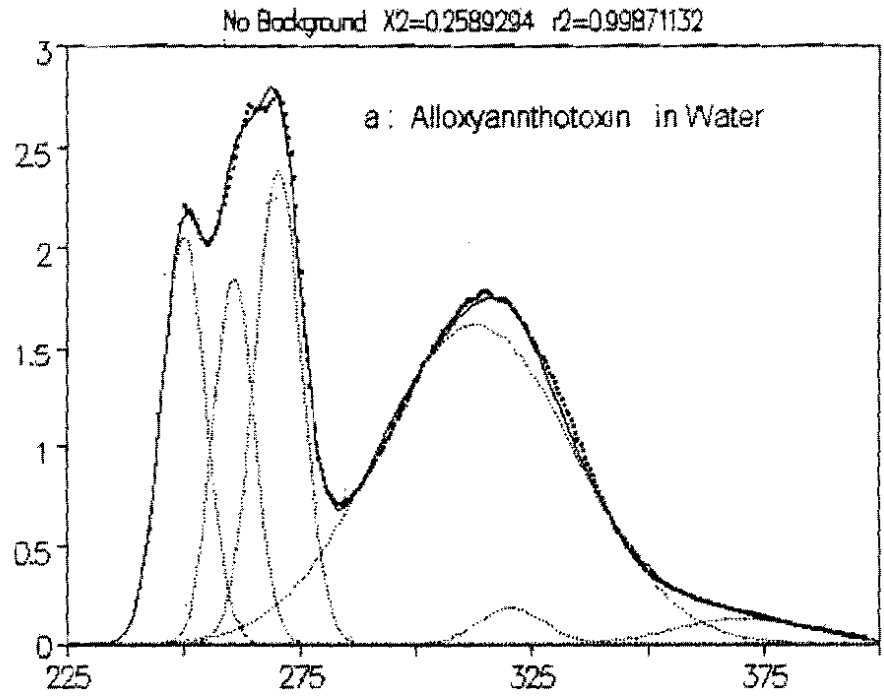
No Background X2=0.2589294 r2=0.99871132
a : Alloxyannthotoxin in Water
3
2.5
2
1.5
1
0.5
0
225
275
325
375

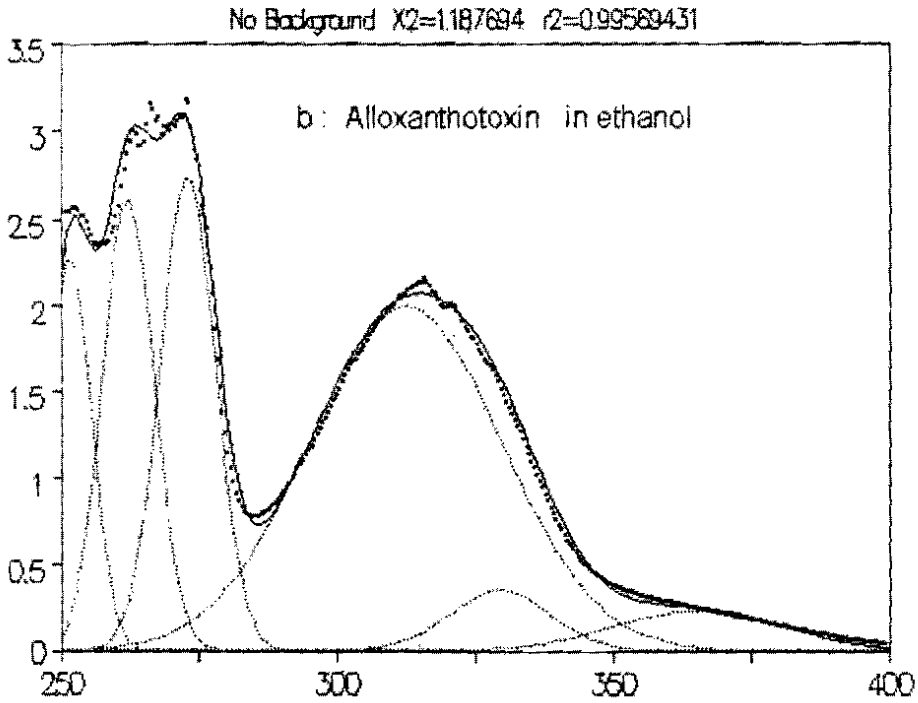
No Background X2=1.187694 r2=0.99569431
b : Alloxanthotoxin in ethanol
3.5
3
2.5
2
1.5
1
0.5
0
250
300
350
400

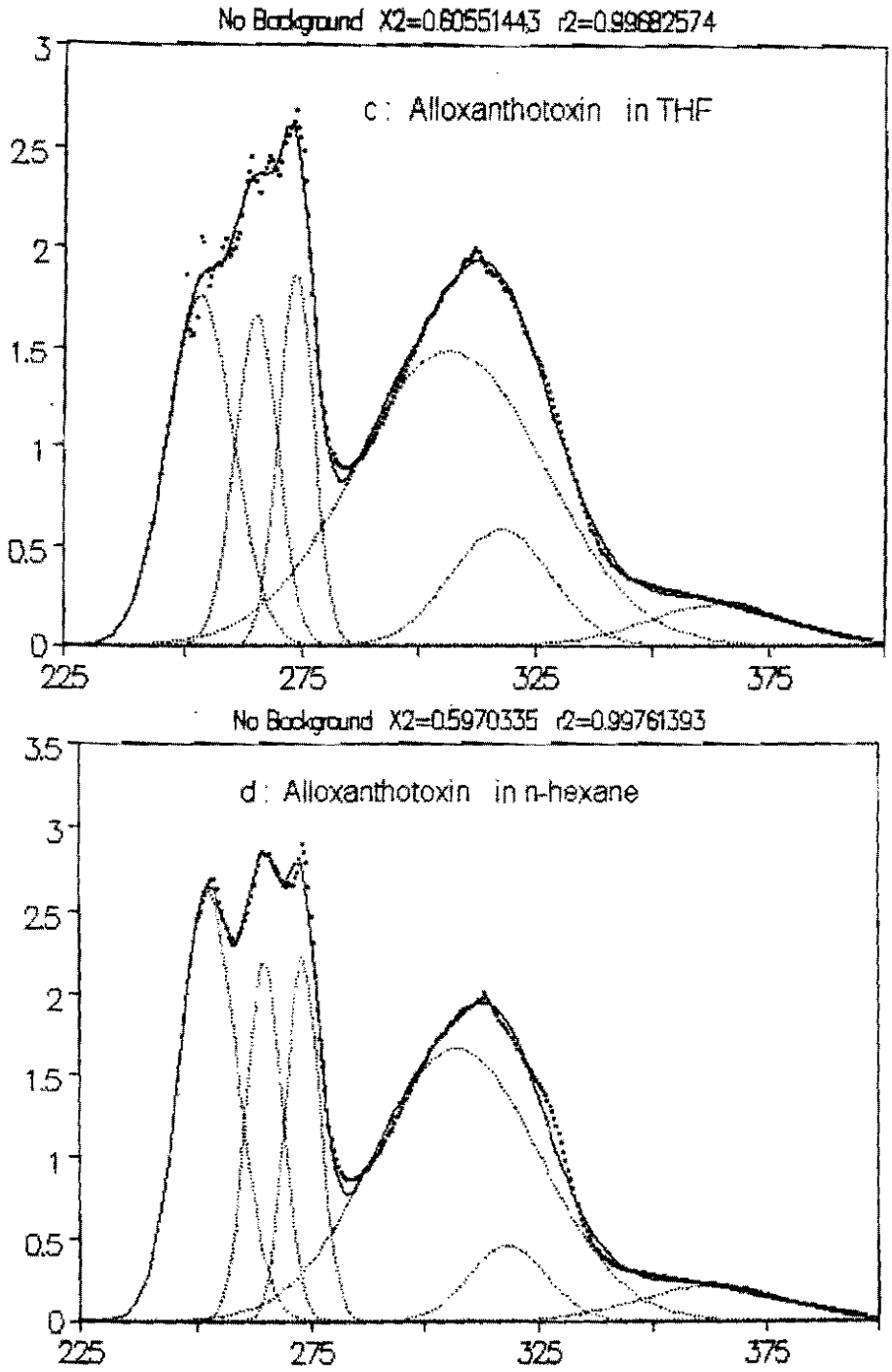

Fig. 9a-d: The Gaussian analysed UV-spectra of alloxanthotoxin (4) in different solvents.

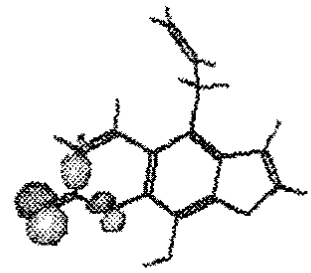

MO 41 E = -10.245 eV

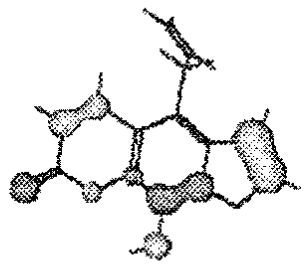

MO 42 E = -9.997 eV

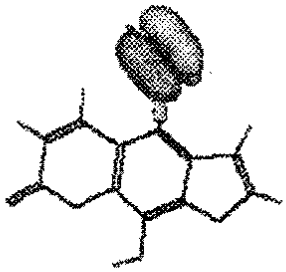

MO 43 E = -9.901 eV

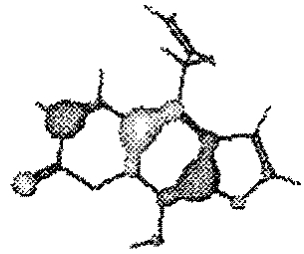

MO 44 E = - 8.366 eV

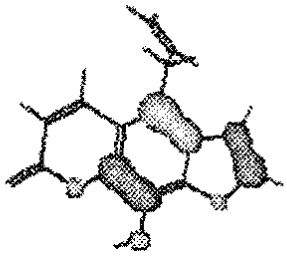

MO 45 E = - 8.117 eV

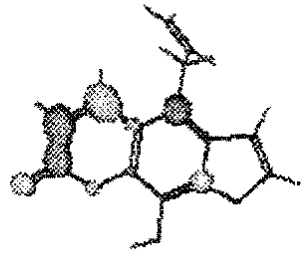

MO 46 E = - 0.702 eV

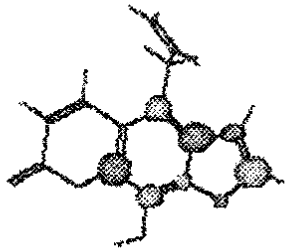

MO 47 E = - 0.025 eV

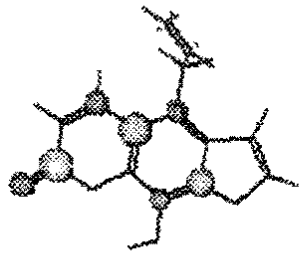

MO 48 E = 0.685 eV

Fig.10: Representation of the calculated wavefunctions of the Molecular Orbitals involved in the electronic transitions of alloxanthotoxin (4). (Orbital contours values less than 0.07 were neglected)

EXPERIMENTAL

Materials :

Xanthotoxin **(1)** was supplied by Memphis Chemical Co., Cairo, Egypt. The known compound xanthotoxol **(2)** was prepared according to literature procedure (Schnberg and Sina, 1953).Allyl bromide **(3)** m.p : 119 b.p : 70-71 supplied by Aldrich fine Chemical Company. **(4)** All solvents used in UV-measurements were spec-pure quality supplied by Merk Chemical Company.

Equipments:

- Melting points were uncorrected and recorded on Reichert thermover apparatus.
- IR spectra were performed on a Unicam SP 2000 Infrared Spectrophotometer using KBr disk technique.
- ^{1}H NMR spectra were measured on JNM-LA-400 MHz, NMR apparatus with $CDCl_3$ as solvent.
- MS spectra were recorded on MS-JEOL-JMS600.
- The photolysis apparatus used wide spectrum medium pressure mercury Lamp (HRI-T250 W). Silica gel 60 GF 254 used in TLC from Merck.
- The electronic absorption spectra of the title compounds (1x10-4 M) was measured in different solvents (pure grade) using Perkin Elmer Lambada 2 absorption spectrophotometer.

Preparation of: 9-Allyloxyfuro[3,2-g][1]benzopyran-2-one (3):

A solution of xanthotoxol **(2)** (4g, 0.0046 mole), allyl bromide (4 g, 0.0085 mole) and potassium carbonate anhydrous (8 g) in acetone (30 ml) was refluxed for 6 hours. The inorganic salts that separated were filtered off. Acetone solution was evaporated under reduced pressure to give a gummy material, which was recrystallized from a mixture of ethyl acetate : n hexane (1:1) to give (3.2g, 80% yield) of a pale brown crystals of **3**, m.p. 75°C. IR(KBr): cm^{-1} = 3090, 2940, 1660, 1600, 1500, 1200 and 1100. ^{1}H-NMR($CDCl_3$): δ = 5.26 (d, J = 6Hz, 2H, CH_2-1'), [ABX system, δ_A = 5.45 (dd, J_{AB} = 2 Hz, J_{AX} = 10 Hz, 1H, H-3'), 5.66 (dd, J_{AB} = 2 Hz, J_{BX} = 16 Hz, 1H, H-3'), 6.41 (comp. pat., 1H, H-2')], 6.60 (d, J = 12 Hz, 1H, H-6), 7.06 (d, J = 2 Hz, 1H, H-3), 7.57 (s, 1H, H-4), 7.92 (d, J = 2 Hz, 1H, H-2) and 8.01 (d, J = 12 Hz, 1H, H-5). MS, R.T. = 2:10 min., m/z = 242.9 (M^+, $C_{14}H_{10}O_4$) (2.2%), 215.9 (M^+-C_2H_3) (1%), 202.9 (M^+-C_3H_4) (38%), 201.9 (M^+-C_3H_5) (24.8%), 200 (M^+-C_3H_7) (100%), 173.9 ($C_{10}H_5O_3$) (20%) and 147.0 ($C_8H_3O_3$) (1%).

Preparation of:4-Allyl-9-hydroxyfuro[3,2-g][1]benzopyran-2-one (4):

The compound was prepared by two different methods

Method A : Thermolysis:

Allyloxy-derivative (**3**) (2g, 0.0083 mole) was fused at 150°C for 30 min., whereas it was melted, resolidified and then melted again. The crude product was recrystallized from ethanol to give colourless crystals of allo-derivative (**4**) (1g, 50% yield), m.p. 208-210°C.

Method B: Photolysis:

A solution of allyloxy derivative (**3**) (0.6g, 0.0025 mole) in $CHCl_3$ (10 ml) was irradiated with ultra violet light in the corning glass test tube without filter at room temperature for 100 hours. The solution was evaporated to dryness to give gummy material which was purified by column chromatography, using silica gel (0.2-0.06 mm), the eluent was petroleum ether 60-80: ethyl acetate (9:1) to give colourless crystals of allo-derivative (**4**) in a poor yield.

IR(KBr): cm^{-1} : 3600, 3140, 2980, 1700, 1670, 1600, 1200 and 1100.

^{1}H-NMR($CDCl_3$): δ = 4.03 (d, J = 6Hz, 2H, CH_2-1'), [ABX system, δ_A = 5.14 (dd, J_{AB} = 2Hz, J_{AX} = 16Hz, 1H, H-3'), δ_B = 5.35 (dd, J_{AB} = 2Hz, J_{BX} = 10Hz, 1H, H-3'), δ_X = 6.21 (comp. pat., 1H, H-2')], 6.45 (d, J = 12Hz, 1H, H-6), 7.10 (d, J = 2Hz, 1H, H-3), 7.52 (s, 1H, OH), 7.95 (d, J = 2Hz, 1H, H-2) and 8.25 (d, J = 2Hz, 1H, H-5).

MS, R.T. 2 : 50 min., m/z 242.9 (M^+, $C_{14}H_{10}O_4$) (39.4%), 241.8 (M^+-H)(100%), 215 (M^+-C_2H_3) (70.6%), 201 (M^+-C_3H_5) (68.8%).

COMPUTATIONS

The molecular geometry of allyloxyxanthotoxin and Alloxanthotoxin were optimized using the ab-initio MO level of computation. The split valence 6-31G* basis set was employed. The GAMESS **[Gamess program ver 6.0, (1993)]** and HyperChem **[Hyperchem Release ver 6.03, (2000)]** software packages were used for Geometry optimization and all other calculations based on the molecular orbital method. The spectral probabilities and band intensities and the properties of the excited states were computed using the ZINDO/s-CI procedure **[Delbene and Jaffe, (1968), Ellis, (1974), Ridely and Zerner, (1976), Bacon and Zerner, (1979)]**. The Origin ver 6.0 package (Gaussin analysis program) was that used for gaussian band-analysis and curve-fitting. All calculations were carried out using IBM-Pentium III-1200 MHz Computer machine.

REFERENCES

A. Schonberg and G. Sina, J. Am. Chem. Soc., **75**, 3265 (1953).

A.D. Bacon and M.C. Zerner, Theor. Chim. Acta, **53**, 21 (1979).

A.M. Zobel and S.A. Brown, Can. J. Bot., **67**, 915 (1989).

A.M. Zobel, S.A. Brown and R.E. March, Can. J. Bot., **69**, 1673 (1991).

B. Epe, M. Haering, D. Ramaiah, H. Stopper, M.M. Abou-Elzahab, W. Adam and C.R. Saha-Möeller, Carcinogenesis, **14**, 2271 (1993).

B.P. Peters, F.G. Weissman and M.A. Gill, Am. J. Health Syst. Pharm., **57**, 645 (2000).

D. Bethea, B. Fullmer, S. Syed, G. Seltzer, J. Tiano, C. Rischko, L. Gillespie, D. Brown and F.P. Gasparro, J. Derm. Sci., **19** : 2, 78 (1999).

E.A. Abu-Mustafa, F.K.A. El-Bary and M.B.E. Fayes, Planta Medica, **18**, 920 (1970).

F. Dall'Acqua, S.M. Magno, F. Zambon and G. Rodighiero, Photochem. Photobiol., **29**, 489 (1979).

Gamess program , W. Schmidt and Co., Iowa State Univ., together with M.Dupuis and J.A. Montgomry, J. Comput. Chem. **14**, 1347 (1993); URL's: http://classic.chem.msu.su./gran/gamess/index.html. and htttp://quantum-2.chem.msu.ru./gran/gamess/index.html.

Gaussian analysis program, Microcal Origin Ver 6.0, Microcal Software Inc., Northampton, MA 01060 USA. URL.

Hyperchem Release 6.03 (eval) for windows molecular modeling system; Hypercube Inc., Copyright 2000; URL : http://hyper.com.

J. Delbene and J. J. Jaffe, J. Chem. Phys. **48**,1807 (1968).

J. E. Ridely and M.C. Zerner, Theor. Chim. Acta, **42**, 223 (1976).

Jing-Xi Pan, Zhen-Hui, Jin Ling Miao, Si-De Tao Nian-Yun Lin and Da-Yuan Zhu, Biophysical Chem., **91** , 105-113 (2001).

L. Swain and K.R. Downum,J. Am. Chem. Soc., 361 (1991).

M.M. Abou-Elzahab, W. Adam and C.R. Saha-Moeller, Liebigs Ann. Chem., 967 (1991).

R.H. Ellis , G. Huehnlenz and J. J. Jaffe, Theor. Chim. Acta **35**, 33 (1974).

تحضير ، فراغى ، الاطياف الايكترونية للفيوروكومارينات الجديدة : الاليلوكسى زانسوتكسين ، الالوزانسوتكسين

أيمان الجندي ، ممدوح سليمان

كلية التربية النوعية – جامعة المنصورة – المنصورة – مصر

كلية العلوم – جامعة المنصورة – المنصورة – مصر

تـم تحضير مشتق الاليلوكسي زانسوتكسين (٣) من مركب الزانسوتكسين الطبيعي مـع مركـب الاليل بروميد. ومن جهه اخري ، عند تعرض المشتق ٣ لدرجة حرارة ١٥٠ درجـة مـئوية تم تحويلة الي مشتق الالوزانسوتكسين (٤) والذى تم تحضيرة ايضا بواسطة تعـرض المركب ٣ للاشعة فوق البنفسجية لمدة ١٠٠ ساعة عند درجة حرارة الغرفة. وقد تمـت دراسة الشكل الفراغي للمركبين ٣ ، ٤ نظريا. وايضا تمت دراسة الطيف الاليكتروني للمركبيـن ٣ ، ٤ فـي المذيبات مختلفة القطبية ، وقد تمت دراسة منحني الامتصاص نظريا بواسـطة بـرنامج جوسن حيث تم مناقشة مختلف مستويات الطاقة للمركبان ٣ ، ٤ . وذلك باستخدام طريقة الزندو – اس كونتم ميكانك.